2013

A Search for RR Lyrae Stars in Segue 2 and Segue 3

Erin Boettcher '12
Class of 2012, Haverford College

Beth Willman
Haverford College, bwillman@haverford.edu

Mariah Baker '14
Class of 2014, Haverford College

Erica Hopkins '14
Class of 2014, Haverford College

Emily Cunningham '12
Class of 2012, Haverford College

See next page for additional authors

The Astronomical Journal, 146:94 (9pp), 2013 October doi:10.1088/0004-6256/146/4/94

A SEARCH FOR RR LYRAE STARS IN SEGUE 2 AND SEGUE 3

Erin Boettcher[1,2], Beth Willman[2], Ross Fadely[2,3], Jay Strader[4], Mariah Baker[2], Erica Hopkins[2], Tonima Tasnim Ananna[5], Emily C. Cunningham[2,6], Tim Douglas[2,7], Jacob Gilbert[2], Annie Preston[2], and Andrew P. Sturner[2,8]
[1] Department of Astronomy, University of Wisconsin, Madison, WI 53706, USA; boettche@astro.wisc.edu
[2] Department of Astronomy, Haverford College, Haverford, PA 19041, USA; bwillman@haverford.edu
[3] Center for Cosmology and Particle Physics, Department of Physics, New York University, New York, NY 10003, USA
[4] Department of Physics and Astronomy, Michigan State University, East Lansing, MI 48824, USA
[5] Department of Physics, Bryn Mawr College, Bryn Mawr, PA 19010, USA
[6] Department of Astronomy and Astrophysics, University of California, Santa Cruz, CA 95064, USA
[7] Dropbox Inc., 185 Berry Street, Suite 400, San Francisco, CA 94107, USA
[8] Laboratory for Atmospheric and Space Physics, University of Colorado, Boulder, CO 80303, USA
Received 2012 August 6; accepted 2013 August 7; published 2013 September 11

ABSTRACT

We present an extensive search for RR Lyrae (RRL) stars in and around the ultra-faint Milky Way companions Segue 2 and Segue 3. The former ($M_V = -2.5$) appears to be an extremely faint dwarf galaxy companion of the Milky Way. The latter ($M_V = 0.0$) is among the faintest star clusters known. We use B and V band time-series imaging obtained at the WIYN 0.9 m telescope at Kitt Peak National Observatory to search for RRL in these objects. In our Segue 2 observations, we present a previously unknown fundamental mode (RRab) RRL star with a period of $P_{\rm ab} = 0.748$ days. With this measurement, we revisit the inverse correlation between $\langle P_{\rm ab}\rangle$ and $\langle[{\rm Fe/H}]\rangle$ established in the literature for Milky Way dwarf galaxies and their RRL. In this context, the long period of Segue 2's RRab star as well as the known significant spread in metallicity in this dwarf galaxy are consistent with the observed trend in $\langle P_{\rm ab}\rangle$ and $\langle[{\rm Fe/H}]\rangle$. We derive the first robust distance to Segue 2, using both its RRab star and spectroscopically confirmed blue horizontal branch stars. Using [Fe/H] $= -2.16$ and -2.44 dex, we find $d_{\rm RRL} = 36.6^{+2.5}_{-2.4}$ and $37.7^{+2.7}_{-2.7}$ kpc; assuming [Fe/H] $= -2.257$ dex, we find $d_{\rm BHB} = 34.4 \pm 2.6$ kpc. Although no RRL were present in the Segue 3 field, we found a candidate eclipsing binary star system.

Key words: galaxies: dwarf – galaxies: star clusters: general – stars: distances – stars: variables: general – techniques: photometric

Online-only material: color figures

1. INTRODUCTION

Over the last decade, numerous ultra-faint ($M_V \gtrsim -8$) companions of the Milky Way have been discovered in Sloan Digital Sky Survey (SDSS) data (e.g., Belokurov et al. 2006, 2007, 2008, 2009, 2010; Koposov et al. 2007; Walsh et al. 2007; Willman et al. 2005a, 2005b; Zucker et al. 2006a, 2006b). Among these discoveries are the least luminous star clusters known (e.g., Koposov et al. 2007; Belokurov et al. 2010; Muñoz et al. 2012), as well as the least luminous, most metal-poor, and most dark-matter-dominated galaxies known (e.g., Kirby et al. 2008; Wolf et al. 2010; Koposov et al. 2011; Simon et al. 2011; Willman et al. 2011). Due to these satellites' low luminosities, it is difficult to determine their distances, dynamical states, and stellar populations. The use of RR Lyrae (RRL) stars as standard candles found in time-series observations has provided an alternative to isochrone fitting for measuring satellite distances.

RRL stars are short-period (0.3–1.0 days, RRab; 0.1–0.55 days, RRc) pulsating variable stars that are found in old and metal-poor stellar populations (Smith 1995; Vivas et al. 2004; Sesar et al. 2007). They are standard candles with mean absolute V band magnitudes of $M_V = 0.59 \pm 0.03$ for [Fe/H] $= -1.5$ (Cacciari & Clementini 2003). RRL stars have been found in considerable numbers in all metal-poor components of the Galaxy; among these RRL are Galactic globular cluster variables as well as field variables in the halo, thick disk, and bulge. RRL stars fall into two distinct regions in period/amplitude space and are thus categorized as fundamental mode (RRab) or first-overtone (RRc) variables whose light curves exhibit characteristic periods, amplitudes, and shapes (Smith 1995). Both types occupy the intersection of the horizontal branch and the instability strip and thus range in color from $B - V = 0.18$ to 0.40; additionally, they display a characteristic increase in $B - V$ at minimum light (Smith 1995).

The QUEST RRL survey found that RRab stars exhibit light curves with mean V band amplitudes of 1.04 ± 0.24 mag and mean periods of 0.539 ± 0.09 days. RRc stars have light curves with mean V band amplitudes of 0.536 ± 0.13 mag and mean periods of 0.335 ± 0.07 days. The former have a distinct saw-toothed shape to their light curves, while the latter have a smoother shape (Vivas et al. 2004). Clement et al. (2001) and Miceli et al. (2008) report mean RRL periods for larger samples of RRL stars in Galactic globular clusters and in the field, respectively. The former studies both RRab and RRc stars and finds mean periods for these populations of 0.585 days and 0.349 days, respectively. The latter studies RRab stars alone and reports a mean period of 0.575 days.

Most of the dwarf companions of the Milky Way, including many of the ultra-faint companions, have been searched for RRL stars. Boötes I, Canes Venatici II, Coma Berenices, Leo IV, and Ursa Major II are among the ultra-faint companions known to host one or more RRL stars (Siegel 2006; Dall'Ora et al. 2006; Kuehn et al. 2008; Greco et al. 2008; Musella et al. 2009; Moretti et al. 2009; Dall'Ora et al. 2012). Segue 1, the least-luminous ($M_V = -1.5$) dwarf galaxy known, has one published RRL star (Simon et al. 2011).

Table 1
Properties of Segue 2 and 3

	Segue 2	Segue 3
R.A. (J2000)	$2^h19^m16^s$	$21^h21^m31^s$
Decl.	$20°10'31''$	$19°07'02''$
M_V	-2.5 ± 0.3	0.0 ± 0.8
$(m - M)_0$	17.7 ± 0.1	16.1 ± 0.1
Half-light radius (r_H)	$3'.4 \pm 0'.2$	$26'' \pm 5''$

Notes. Values for Segue 2 are from Belokurov et al. (2009) and values for Segue 3 are from Fadely et al. (2011).

Segue 2 ($M_V = -2.5 \pm 0.3$; Belokurov et al. 2009) and Segue 3 ($M_V = 0.0 \pm 0.8$; Fadely et al. 2011) are two recently discovered ultra-faint companions of the Milky Way (see Table 1 for the properties of these objects). Segue 2 is classified as a dwarf galaxy by Kirby et al. (2013), because of the significant spread in the [Fe/H] of its constituent stars (Willman & Strader 2012). Segue 3 is among the lowest-luminosity star clusters known (Fadely et al. 2011), and shares similar properties with a few other extremely low-luminosity star clusters such as Muñoz 1 (Muñoz et al. 2012). However, its close proximity ($d \approx 17$ kpc) makes it a particularly strong candidate for studying such an extreme stellar system. Additionally, tidal disruption of the object is suggested by the 11 candidate member stars found more than three half-light radii from the center of the object (Fadely et al. 2011). Thus, Segue 3 may be a valuable laboratory for studying the dynamical evolution of such systems.

The accuracy with which the distances to Segue 2 and 3 can be measured affects the accuracy with which many fundamental physical properties can be determined. The distance to Segue 2 is currently estimated using the apparent magnitudes of four candidate blue horizontal branch members (Belokurov et al. 2009). The distance to Segue 3 is determined by performing isochrone fitting to spectroscopically selected members using a maximum likelihood method (Fadely et al. 2011). If one or more RRL stars can be shown to belong to these objects, then they will provide a robust complimentary approach to constraining these distances.

In this paper, we search for RRL stars in and around Segue 2 and 3. In Section 2, we describe the collection and reduction of multi-band time-series observations at the WIYN 0.9 m telescope at Kitt Peak National Observatory (KPNO). Section 3 describes the use of DAOPHOT II and ALLSTAR II to perform point-spread function (PSF) photometry, details the astrometric and photometric calibration, and describes the selection of variable star candidates. In Section 4, we present a fundamental mode RRL star in Segue 2 and a candidate eclipsing binary star system in the Segue 3 field. We use the former as well as three confirmed blue horizontal branch members to determine the distance to Segue 2 and then consider its RRL properties in the context of other Milky Way dwarf galaxies. We conclude with a brief review of our results in Section 5.

2. DATA

2.1. Observations and Data Reduction

We obtained Harris B and V band time-series observations of the Segue 2 and 3 objects using the 0.9 m WIYN telescope and S2KB CCD camera at KPNO. On 2010 October 12 and 13, in gray conditions, we obtained 24 (11 B, 13 V band) images of Segue 2 and 42 (20 B, 22 V band) images of Segue 3. The seeing ranged from $1''.1$ to $2''.6$ with a median seeing of $1''.7$. From 2011 October 8 to 11, in bright conditions, we took 69 (34 B, 35 V band) exposures of Segue 2 and 71 (35 B, 36 V band) exposures of Segue 3. The seeing ranged from $1''.2$ to $3''.2$ with a median seeing of $1''.7$. For Segue 2, the exposure times ranged from 300 to 600 s in B band and 180 to 600 s in V band. For Segue 3, the exposure times varied from 180 to 300 s in both the B and V bands. The exposures were taken alternating between the B and V bands, and the minimum time between subsequent exposures was set by a read-out time of approximately three minutes. The S2KB CCD camera is an array of 2048 × 2048 pixels with a scale of 0.6 arcsec pixel^{-1}. Both Segue 2 ($r_H = 3'.4 \pm 0'.2$; Belokurov et al. 2009) and Segue 3 ($r_H = 0'.43 \pm 0'.08$; Fadely et al. 2011) were fully captured within the $20'$ by $20'$ field of view.

To prepare the images for analysis, the exposures were bias-subtracted, flat-fielded using dome flats, and trimmed to remove the overscan region. The DAOPHOT II and ALLSTAR II packages were used to perform PSF photometry on all of the images (Stetson 1987, 1994). We allowed the PSF to vary quadratically as a function of position. To assess the point source detection completeness of our photometry, we matched stars from the Sloan Digital Sky Survey Data Release 7 (SDSS DR7; Abazajian et al. 2009) to our detected sources within the footprint of our observations. For both the Segue 2 and 3 fields, our photometric catalog includes 100% of SDSS stars brighter than $m_{V,0} \sim 19.5$ mag within our footprint, well below the apparent V band magnitude of the horizontal branches of these objects (see Sections 3 and 4). SDSS DR7 is ∼95% complete to g, $r \sim 22.2$ mag,[9] so we infer a similarly high point source detection completeness for our data. While this comparison with SDSS does not itself account for crowding incompleteness, neither Segue 2 nor Segue 3 are crowded in their central regions. We conclude that it is unlikely that we have missed an RRL star in either Segue 2 or Segue 3 owing to photometric incompleteness, but we cannot rule out the possibility with 100% confidence.

2.2. Astrometric Calibration

The online resource Astrometry.net[10] was used to obtain astrometric headers for each exposure. We accessed Astrometry.net with a Python script to enable automated processing of all exposures. We used this astrometry to facilitate cross-matching sources between the S2KB exposures and also to the SDSS DR7 catalog. Since the astrometry in the SDSS catalog is more precise than we could obtain for our KPNO data, all coordinates reported in this paper come from SDSS DR7.

2.3. Photometric Calibration

The data were photometrically calibrated to SDSS DR7 photometry.[11] We transformed the SDSS g and r magnitudes to B and V using the filter transformations of Jordi et al. (2006). The errors are on the order of a few hundredths of a magnitude for these filter transformations. In the Segue 2 field, the median errors on our standard magnitudes were thus increased from ∼0.018 and 0.017 mag in g and r to ∼0.037 and 0.020 mag in B and V, respectively. For the Segue 3 field, the corresponding values were ∼0.012 and 0.011 in g and r and ∼0.029 and 0.016 in B and V. All magnitudes used for the light curves and distances presented in this paper have been corrected for dust using the

9 http://www.sdss.org/dr7/
10 http://nova.astrometry.net/
11 Downloaded from http://casjobs.sdss.org/CasJobs/.

Table 2
Photometric Calibration Coefficients

	Segue 2	Segue 3
α_B	0.113	0.160
β_B	-4.13×10^{-5}	-6.47×10^{-5}
γ_B	7.25×10^{-5}	6.16×10^{-5}
ζ_B	2.77	2.71
α_V	-0.0620	-0.0505
β_V	-3.52×10^{-5}	-4.45×10^{-5}
γ_V	9.39×10^{-5}	4.47×10^{-5}
ζ_V	3.13	3.04

Notes. Representative values of the photometric calibration coefficients from Equation (2). The β, γ, and ζ terms are medians among all images for each object and filter.

Schlegel et al. (1998, hereafter SFD98) maps (assuming $R_V = 3.1$), and using the updated reddening coefficients presented in Schlafly & Finkbeiner (2011). $E(B-V)$ at the center of Segue 2 is 0.183 and at the center of Segue 3 is 0.099.

We used a maximum likelihood analysis to calibrate our data to SDSS as a function of color, x-pixel position, and y-pixel position. We maximize the log-likelihood:

$$\ln \mathcal{L} = -\frac{1}{2}\sum_i\sum_j\left(\left[\frac{(m_{\mathrm{SDSS},j} - m_{\mathrm{mod},ij})^2}{\sigma_{ij}^2}\right] + \ln \sigma_{ij}^2\right) \quad (1)$$

where:

$$m_{\mathrm{mod},ij} = m_{\mathrm{instr},ij} + \alpha(B-V)_{\mathrm{SDSS},j} + \beta_i x_{i,j} + \gamma_i y_{i,j} + \zeta_i \quad (2)$$

and:

$$\sigma_{i,j}^2 = \sigma_{\mathrm{SDSS},j}^2 + \sigma_{\mathrm{instr},ij}^2 + (\alpha\sigma_{B-V,j})^2. \quad (3)$$

Here, i refers to the image number and j to the star number. $m_{\mathrm{instr},ij}$ and $\sigma_{\mathrm{instr},ij}$ are the instrumental magnitudes and random uncertainties, $m_{\mathrm{SDSS},j}$ and $\sigma_{\mathrm{SDSS},j}$ are the SDSS magnitudes and uncertainties, $(B-V)_{\mathrm{SDSS},j}$ and $\sigma_{B-V,j}$ are the SDSS colors and uncertainties, and $x_{i,j}$ and $y_{i,j}$ are x- and y-coordinates in pixels. For $\sigma_{\mathrm{instr},ij}$ we use the value reported by the ALLSTAR II software. Thus, a single color term (α) is found for each data set, while a unique x term (β_i), y term (γ_i), and zero point (ζ_i) is found for each exposure. The final α, β_i, γ_i, and ζ_i terms and corresponding uncertainties are taken to be the median and standard deviation of the distributions obtained using a bootstrapping technique. Representative values of α, β, γ, and ζ are shown in Table 2. We apply these terms and propagate their uncertainties into the calibrated data and corresponding uncertainties presented in the remainder of this paper. After the data are calibrated, evidence of small spatially dependent residuals is present in the Segue 3 field (but not in the Segue 2 field). While the variable star in the Segue 3 field presented in Section 4 resides on a part of the chip that appears relatively unaffected, the photometry for the star as presented in Table 3 has an additional systematic uncertainty of a few hundredths of a magnitude.

2.4. Selection of Variable Stars

To select a set of variable star candidates, we quantify the change in magnitude between the ith observation of a given source and the error-weighted, sigma-clipped average magnitude of the source as:

$$\delta_{\mathrm{mag},i} = \left|\frac{\langle m\rangle - m_i}{\sqrt{\sigma_{\langle m\rangle}^2 + \sigma_i^2}}\right| \quad (4)$$

where $\langle m\rangle$ and m_i are the average magnitude and the ith observed magnitude of the source and $\sigma_{\langle m\rangle}$ and σ_i are the uncertainties on these quantities. These include both random and systematic components of the uncertainty. To obtain an initial set of variable star candidates, we selected those stars for which $\delta_{\mathrm{mag},i} \geqslant 3.0$ for at least three exposures in either passband and from any observing epoch, as well as those sources which showed a change in magnitude of greater than 0.5 mag.

We evaluate our ability to identify RRL stars as variable star candidates using these selection criteria by simulating RRL light curves at the cadence and precision of our calibrated observations over the full range of RRL period and amplitude parameter space. We base our simulations on a representative set of 20 RRab and 2 RRc g and r templates provided by Sesar et al. (2010) and transformed to B and V using the transformations of Jordi et al. (2006). The uncertainties are simulated as Gaussian random errors equal to the observed uncertainties (including both random and systematic components) for the RRab star in Segue 2 (see Section 3), and for the candidate eclipsing binary in the Segue 3 field (see Section 4). We use the eclipsing binary for Segue 3 because its color and magnitude are broadly consistent with the instability strip of Segue 3. A total of 45,000 RRab light curves and 2000 RRc light curves were simulated by taking linear steps through period, amplitude, and initial phase of observation. The period was varied from 0.3 to 1.0 days for RRab stars and from 0.1 to 0.55 days for RRc stars (Vivas et al. 2004; Sesar et al. 2007). The amplitude was varied from 0.4 to 1.8 mag and from 0.1 to 1.0 mag for RRab and RRc stars, respectively (Vivas et al. 2004; Sesar et al. 2007).

We define the detection efficiency of our study as our ability to select our simulated RRL stars as variable star candidates using the selection criteria described above. Note that this definition of the detection efficiency only assesses our ability to flag a source as a variable star candidate for further evaluation. It does not aim to assess the accuracy with which we recover the source's input parameters (period, amplitude, etc.) through means such as light curve template fitting. Thus, our detection efficiency mainly assesses whether the cadence of our observations allows for sufficient sampling of RRL light curves to be able to use the selection criteria defined above to identify these light curves as variable.

In Segue 3, nearly all of our simulated RRL were identified as variable star candidates for all periods and amplitudes simulated. In Segue 2, our identification of variable stars

Table 3
Properties of Periodic Variables

	Segue 2 Variable	Segue 3 Variable
R.A. (J2000)	$2^{\mathrm{h}}19^{\mathrm{m}}0\overset{\mathrm{s}}{.}06$	$21^{\mathrm{h}}21^{\mathrm{m}}41\overset{\mathrm{s}}{.}21$
Decl.	$20°06'35\overset{''}{.}15$	$19°00'5\overset{''}{.}51$
$\langle m_V\rangle_0$	$18.25^{+0.03}_{-0.02}$	16.86 ± 0.01
$\langle B-V\rangle_0$	0.38 ± 0.012	0.55 ± 0.004
Amplitude (B)	$0.62^{+0.024}_{-0.020}$	~0.45
Amplitude (V)	$0.51^{+0.018}_{-0.015}$	~0.45
Period (days)	$0.748^{+0.006}_{-0.006}$	~0.167
$E(B-V)$	0.220	0.102
Classification	RRab	Candidate eclipsing binary

was similarly successful; however, in several areas of period/amplitude parameter space, $\gtrsim$10% of sources failed to meet our selection criteria. These areas included RRab stars with the lowest amplitudes and longest periods (0.9–1.0 days), as well as those with amplitudes of $\sim$0.4 mag. They also included RRc stars with amplitudes <0.2 mag, with the longest periods again being the least detectable. Given that RRab stars with periods greater than 0.9 days are rare (Miceli et al. 2008; Vivas et al. 2004), as are RRc stars with amplitudes below 0.2 mag (Vivas et al. 2004), we are confident that the cadence of our observations combined with our selection criteria are sufficient for successfully identifying RRL stars as variable star candidates.

In our Segue 2 and 3 observations, approximately 3% and 2% of stars were selected as variable star candidates, respectively. The raw light curves of these candidate variable stars (magnitude versus HJD) were then visually inspected with particular attention paid to stars that varied in both *B* and *V* band, varied throughout the observing period, and/or showed potentially periodic changes in magnitude. The vast majority of variable star candidates were falsely identified as variable due to outliers in otherwise flat light curves, significant scatter in faint light curves, or proximity to other sources or to the edges of the exposures. A smaller number of stars ($\sim$3 per field) showed non-periodic variation over some or all of the observing period. Although further observation of these stars may inform our understanding of the stellar populations in and around Segue 2 and 3, their lack of periodic variation eliminated them from consideration as RRL stars. Finally, as discussed in Section 4, one clear periodic variable star was identified in each of the Segue 2 and 3 fields.

3. A RR LYRAE IN SEGUE 2

A periodic variable star was detected in Segue 2 at (R.A., decl.) = $(2^{\rm h}19^{\rm m}0\overset{\rm s}{.}06, 20^\circ06'35\overset{''}{.}15)$ at a distance of 1.6 half-light radii from the center of the object. This star was found to be a spectroscopic member of Segue 2 by Kirby et al. (2013). The variable has a period, amplitude, and sawtooth-shaped light curve consistent with that of a fundamental mode RRL star (RRab). As shown in Figure 1, the variable has a color and magnitude consistent with being an RRL member of Segue 2 based on past measurements of the distance to Segue 2 (see Belokurov et al. 2009) and KPNO and SDSS photometry of the object.

To deduce the properties of the variable's light curve, we fit our observed *B* and *V* light curves with the RRab and RRc light curve templates of Sesar et al. (2010). The set consists of approximately 20 RRab and 2 RRc *ugriz* templates that span a distribution of light curve shapes derived from observations. The SDSS *g* and *r* magnitudes of the templates were transformed to *B* and *V* using the filter transformations of Jordi et al. (2006). For all 420 RRab templates, we initially explored period and amplitude parameter space by conducting gridded searches for a minimum χ^2 fit. As the template fitting was performed separately in the *B* and *V* bands, we define the χ^2 value of a template fit as the sum of the χ^2 values of its *B* and *V* band fits. We selected eight RRab templates as providing the most reasonable fits to the data (i.e., $\chi^2 \lesssim 70$). These templates were used to explore the range of possible periods and amplitudes using `emcee`,[12] a Markov Chain Monte Carlo (MCMC) routine (Foreman-Mackey et al. 2013).

[12] http://danfm.ca/emcee/

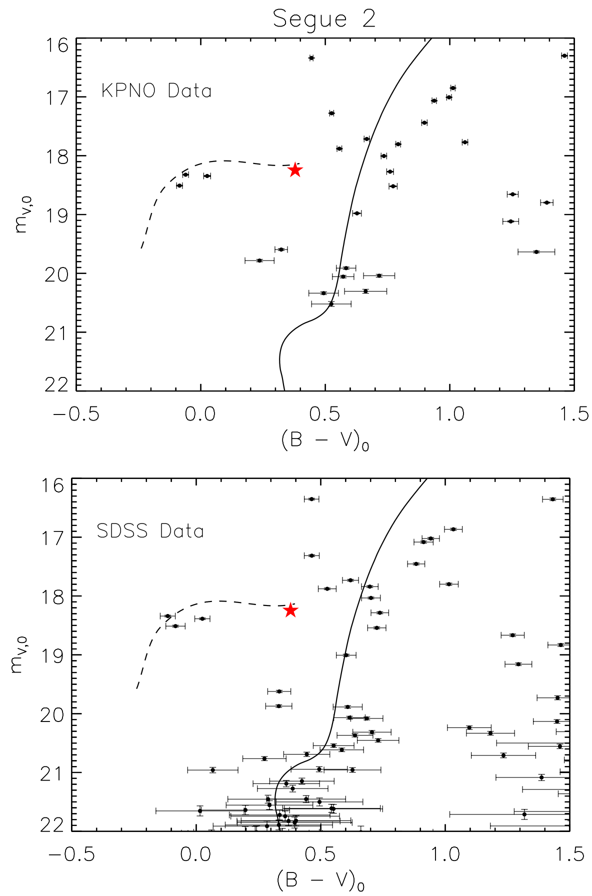

Figure 1. Location of the RRab star along the horizontal branch of Segue 2 is shown in KPNO and SDSS photometry of the Segue 2 field within 1 half-light radius of the center of the object. The KPNO photometry of the variable is indicated by a red star. The isochrone (solid line) and horizontal branch fiducial (dashed) have [Fe/H] = −2.257 and d = 37.0 kpc. Although these are overlaid to guide the eye, isochrone fitting was not performed due to the small number of sources belonging to the object and the high level of contamination from sources in the field. The isochrone was obtained from the Dartmouth Stellar Evolution Database (see http://stellar.dartmouth.edu/models/index.html), and the horizontal branch fiducial is a metallicity-corrected combined M3 and M13 fiducial from Sand et al. (2012).

(A color version of this figure is available in the online journal.)

For each template, the MCMC sampling returns the posterior distribution of the period and amplitude. We find a bi-modal distribution of periods and amplitudes consisting of a primary and secondary peak in the parameter space. Although the template fitting was performed separately in the *B* and *V* bands, we selected a single best-fit template having the minimum sum of its χ^2 values in *B* and *V*. For the primary peak among RRab templates, this best-fit template gives a period of $P = 0.748^{+0.006}_{-0.006}$ days, a *B* band amplitude of $A_B = 0.623^{+0.024}_{-0.020}$ mag, and a *V* band amplitude of $A_V = 0.509^{+0.018}_{-0.015}$ mag. At a 68% confidence level, the other seven templates are in good agreement with the first, providing periods as short as 0.742 days and as long as 0.769 days, *B* band amplitudes that range from 0.596 to 0.667 mag, and *V* band amplitudes that range from 0.493 to 0.564 mag. For the secondary peak, the MCMC samples imply a shorter period ($P = 0.414^{+0.006}_{-0.002}$ days) and smaller amplitude ($A_V = 0.475^{+0.043}_{-0.043}$). However, the light curve templates in this peak yield much larger χ^2 values than in the primary peak, and a visual comparison of the light curves and the data reveals them to provide a poor match. Furthermore, Lomb-Scargle periodograms constructed for both bandpasses suggest a most probable period of $P \sim 0.735$ days, which is broadly consistent with the period of the primary peak.

Additionally, we assessed the likelihood that the variable could instead be an RRc star by exploring period and amplitude parameter space with `emcee` using two RRc templates. However, the RRc templates generally yield large χ^2 values and poor visual matches to the data. The only RRc template fits that have χ^2 values comparable to the RRab fits in the primary peak have periods on the order of 0.75 days, much longer than expected for this class of variable. Thus, this star does not meet the characteristic profile of an RRc star.

Figure 2 shows the variable's period folded B_0, V_0, and $(B - V)_0$ light curves, with the best fit template overplotted. By integrating the set of light curve templates consistent with the observed light curve at a 68% confidence level or better, we calculate a flux-averaged B band magnitude of $\langle m_B \rangle_0 = 18.620^{+0.046}_{-0.021}$ mag and a flux-averaged V band magnitude of $\langle m_V \rangle_0 = 18.246^{+0.032}_{-0.020}$ mag. While using this approach provides a reasonable estimate of the uncertainty in $\langle m_B \rangle_0$ and $\langle m_V \rangle_0$, the resulting uncertainty bars on the magnitudes are not themselves formal 68% confidence intervals. The star has a median color of $\langle B - V \rangle_0 = 0.379 \pm 0.012$ and varies in color from $(B - V)_0 \approx 0.27$ to $(B - V)_0 \approx 0.51$ over the course of the pulsational period, displaying the increase in $B - V$ at minimum light that is characteristic of RRL stars (Smith 1995).

It should be noted that the point-to-point scatter in these light curves appears smaller than expected given the size of the error bars, which include both random and systematic uncertainties. This small point-to-point scatter suggests that the random uncertainties are overestimated by ALLSTAR II and/or the systematic uncertainties are highly correlated from exposure-to-exposure. The systematic uncertainties account for up to 50% of the error. Although the systematics are likely correlated, we chose to include them in the error bars because they are derived separately for each exposure and because they must be included in the error budget for the RRL's distance estimate in Section 3.2.

3.1. *Comparison with the RRL Properties of Other Milky Way Dwarf Galaxies*

Here, we briefly discuss Segue 2's RRL star in the context of the RRL populations of other Milky Way dwarf galaxy companions. Historically, RRab stars in the Milky Way's halo, globular clusters, and dwarf galaxies have been classified according to their Oosterhoff properties (Oosterhoff 1939). RRab stars with short periods and large amplitudes are classified as Oosterhoff I (OoI) stars, and those with longer periods and smaller amplitudes are deemed Oosterhoff II (OoII) stars. Milky Way globular clusters are known to show an Oosterhoff gap, or an absence of clusters with $0.58 \lesssim \langle P_{ab}$ (days)$\rangle \lesssim 0.62$. However, Milky Way dwarf galaxies do not display this same dichotomy, and instead largely fall in the Oosterhoff intermediate to OoII classifications (see, e.g., Catelan 2009).

Among Galactic globular clusters, an OoII classification is associated with the most metal-poor systems ([Fe/H] < -1.5), with a weak negative correlation between the mean RRab period and metallicity (Catelan 2009). For dwarf galaxies of the Milky Way, which are also metal-poor, a similar correlation between $\langle P_{ab} \rangle$ and $\langle$[Fe/H]$\rangle$ also exists (see, e.g., Smith et al. 2009; Catelan 2009; Clementini 2010).

To place the Oosterhoff classification and long period of Segue 2's RRab star in a more specific context, we revisit the

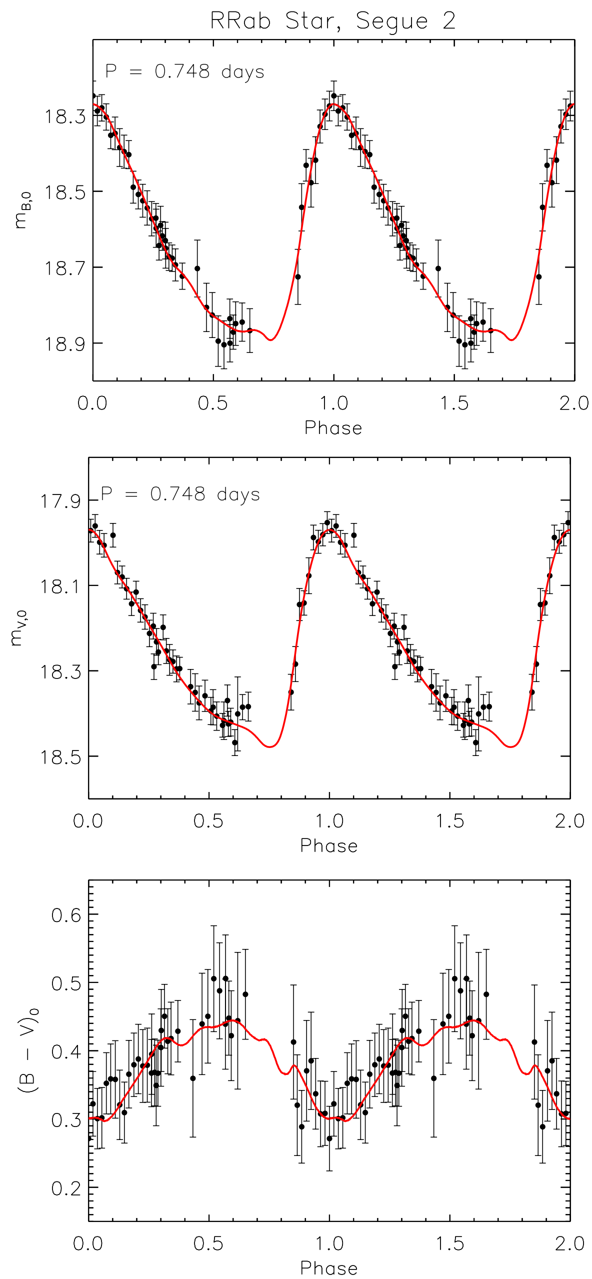

Figure 2. B_0 and V_0 light curves of the fundamental mode RRL star in Segue 2 are shown in the top and middle panels. Overplotted is the best-fit fundamental mode RRL template from Sesar et al. (2010). The B_0 and V_0 light curves have amplitudes of 0.623 and 0.509 mag, respectively. The $(B - V)_0$ light curve shown in the bottom panel displays the increase in $B - V$ at minimum light that is characteristic of RRL stars. The error bars include both random and systematic uncertainty.

(A color version of this figure is available in the online journal.)

relation between mean RRab period and mean metallicity for dwarf galaxies using homogeneously calculated values obtained with a method that remains robust for ultra-faint systems whose metallicity distributions may be poorly sampled. We use the uniformly calculated set of $\langle$[Fe/H]$\rangle$ and associated uncertainties found by Willman & Strader (2012) by applying a Bayesian MCMC technique to published [Fe/H] measurements based on iron lines and their accompanying uncertainties. A similar technique was applied to recalculate $\langle P_{ab} \rangle$ and associated uncertainties from the most current surveys of variable stars in ultra-faint dwarfs.

Table 4
⟨[Fe/H]⟩ and $\langle P_{ab} \rangle$ for Milky Way Dwarf Companions

Object	N_{RRab}[a]	⟨[Fe/H]⟩	$\sigma_{\langle [Fe/H] \rangle}$	$\langle P_{ab} \rangle$	$\sigma_{\langle P_{ab} \rangle}$	$\langle P_{ab} \rangle$ ref	⟨[Fe/H]⟩ Ref
CVn I	18	−1.962	0.038	0.600	0.006	Kuehn et al. (2008)	WS12, K10
Herc	6	−2.518	0.140	0.678	0.013	Musella et al. (2012)	WS12, K08
For	396	−1.025	0.012	0.585	0.002	Bersier & Wood (2002)	WS12, K10
Dra	123	−1.946	0.024	0.619	0.004	Bonanos et al. (2004)	WS12, K10
Leo IV	3	−2.363	0.230	0.655	0.028	Moretti et al. (2009)	WS12, K08
Sex	26	−1.966	0.039	0.606	0.010	Mateo et al. (1995)	WS12, K10
Leo I	47	−1.450	0.011	0.602	0.009	Held et al. (2001)	WS12, K10
Leo II	103	−1.670	0.024	0.620	0.006	Siegel & Majewski (2000)	WS12, K10
UMi	47	−2.112	0.027	0.638	0.009	Nemec et al. (1988)	WS12, K10
Scl	129	−1.726	0.024	0.584	0.007	Kaluzny et al. (1995)	WS12, K10
Boo I	7	−2.531	0.132	0.691	0.034	Siegel (2006)	Norris et al. (2010)
ComBer	1	−2.640	0.100	0.670	···	Musella et al. (2009)	WS12, K08
CVn II	1	−2.444	0.178	0.743	···	Greco et al. (2008)	WS12, K08
UMa I	5	−2.334	0.128	0.628	0.032	Garofalo et al. (2013)	WS12, K08
UMa II	1	−2.357	0.204	0.659	···	Dall'Ora et al. (2012)	WS12, K08
Seg2	1	−2.257	0.140	0.748	···	present work	Kirby et al. (2013)[b]

Notes. WS12, Willman & Strader (2012); K08, Kirby et al. (2008); K10, Kirby et al. (2010). When two references are listed for ⟨[Fe/H]⟩, the WS12 reference contains the calculated average and uncertainty and the K08 or K10 reference contains the original [Fe/H] measurements.

[a] As the cited RRL surveys are not necessarily complete for the more luminous dwarfs, the number of RRab stars cited as belonging to these dwarfs may be underestimated. Additionally, RRab stars with abnormal or uncertain classifications were not included in the total count.

[b] The mean metallicity of Segue 2 was calculated using the technique described in Willman & Strader (2012) from the individual metallicities published in Kirby et al. (2013).

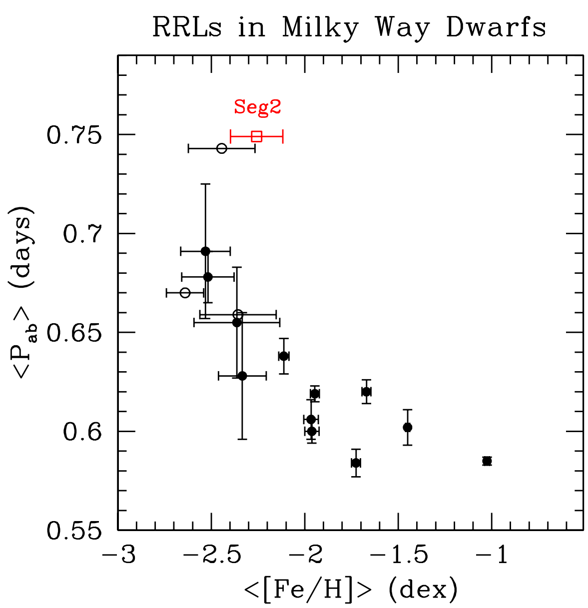

Figure 3. Mean RRab period vs. mean [Fe/H] for Milky Way dwarf galaxies with predominately old stellar populations. The error bars are uncertainties in the means. The filled circles show galaxies with multiple RRab stars; the open circles show objects with either one RRab star or for which individual periods are unavailable, so that these points have no formal uncertainty in the mean period. The long RRab period and mean metallicity of Segue 2 are consistent with the established trend in $\langle P_{ab} \rangle$ and ⟨[Fe/H]⟩ given the significant spread in metallicity established for Segue 2 by Kirby et al. (2013). The data and sources are listed in Table 4.

(A color version of this figure is available in the online journal.)

In Figure 3, we compare Segue 2's RRab period and mean metallicity with those of other Milky Way dwarf galaxies with predominantly old stellar populations. The long period ($P_{ab} = 0.748$ days) and the amplitude ($A_V = 0.509$ mag) of Segue 2's RRab star as well as the dwarf galaxy's mean metallicity (⟨[Fe/H]⟩ = −2.257) are consistent with an OoII classification (see, e.g., Kunder et al. 2011). The periods of the single RRL star in each of Segue 2 and CVn II are longer than the (mean) RRab period of any other dwarf galaxy. However, the period of the RRab star in Segue 2 and the mean metallicity of the dwarf galaxy are consistent with the strong anti-correlation between $\langle P_{ab} \rangle$ and ⟨[Fe/H]⟩ observed in dwarfs given the significant spread in [Fe/H] confirmed by Kirby et al. (2013).

We can also compare the RRL populations of Milky Way dwarf galaxy companions using the RRL specific frequency S_{RR}, or the number of RRL stars per system normalized to a system absolute magnitude of $M_V = -7.5$:

$$S_{RR} = N_{RR} 10^{0.4(7.5+M_V)}. \quad (5)$$

Given its one RRL star and an absolute magnitude $M_V = -2.5$ (Belokurov et al. 2009), Segue 2 has an RRL specific frequency $S_{RR} = 100$. Using the absolute magnitudes provided in Sand et al. (2012), we find that this is greater than the specific frequency of any other Milky Way dwarf galaxy companion considered in Table 4. These objects have S_{RR} values that range from ∼1.3 (Leo I) to ∼60.4 (ComBer). Of the known dwarf companions, only Segue 1 ($M_V = -1.5$), which is known to have at least one RRL star (Simon et al. 2011), appears to have a higher RRL specific frequency. It is necessary to note that as the completeness of the RRL surveys in these objects is not guaranteed, the specific frequencies of these objects are lower limits. Nevertheless, it is interesting to observe that Segue 2 may have a high specific frequency compared to most other dwarf galaxy companions in which RRL stars have been discovered.

3.2. Distance to Segue 2

We calculate the distance to Segue 2 using both its newly identified RRL star and its blue horizontal branch (BHB) stars (with the technique described in Section 3 of Sand et al. 2012). As described in Section 2.3, we used the Schlafly & Finkbeiner (2011) reddening coefficients rather than the SFD98 coefficients for the photometry used to calculate these distances. For both

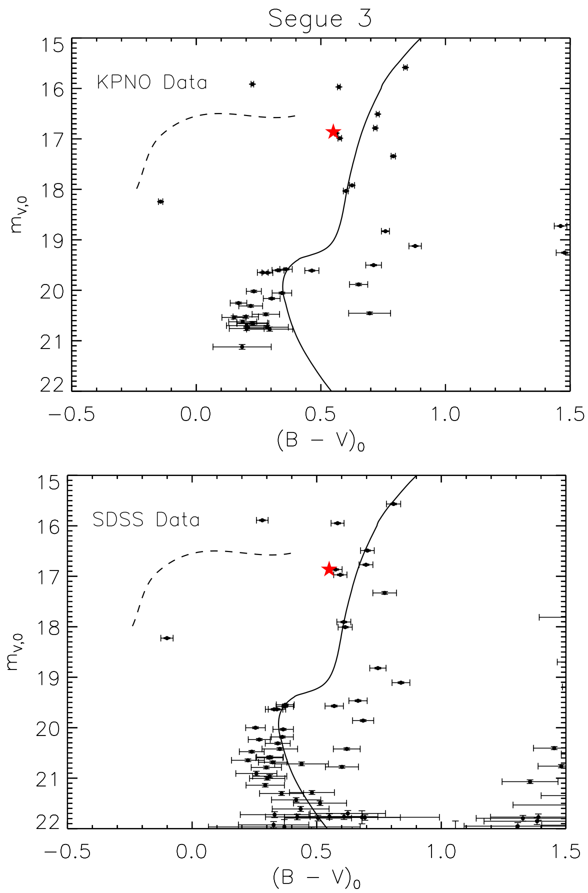

Figure 4. Variable star in the Segue 3 field is consistent in magnitude but not in color with the horizontal branch of Segue 3 as indicated by KPNO and SDSS photometry of the object within 3 half-light radii of the center. The KPNO photometry of the variable is indicated by a red star. The isochrone (solid line) and horizontal branch fiducial (dashed) have [Fe/H] = −1.7 and $d = 16.9$ kpc and were obtained from the same sources as those in Figure 1.

(A color version of this figure is available in the online journal.)

the RRL and the BHB technique, the updated coefficients make the inferred distance to Segue 2 several percent larger than it would have been with the SFD98 coefficients.

Using either the RRL star or BHB stars to calculate the distance to Segue 2 requires knowledge of the stars' metallicities. Using the individual metallicities of member stars from Kirby et al. (2013), we calculate a mean metallicity of [Fe/H] = -2.257 ± 0.140 (as described in Section 3.1). The BHB [Fe/H] value estimated by Belokurov et al. (2009) is consistent with this value. Using the three BHB members and [Fe/H] = −2.257, we find a distance to Segue 2 of $d = 34.4 \pm 2.6$ kpc.

To calculate the RRL distance, we first estimate the metallicity of the RRL star using each of the following relationships between RRab metallicity, period, and V band amplitude:

$$[\mathrm{Fe/H}] = -8.85[\log P_{\mathrm{ab}} + 0.15 A_V] - 2.60 \quad (6)$$

$$[\mathrm{Fe/H}] = -3.43 - 7.82 \log P_{\mathrm{ab}}. \quad (7)$$

The former relation, from Alcock et al. (2000), and the latter, from Sarajedini et al. (2006), have estimated uncertainties of approximately 0.31 and 0.45 dex, respectively. Using $P_{\mathrm{ab}} = 0.748$ days and $A_V = 0.509$ mag, we find [Fe/H] values of −2.16 and −2.44 dex.

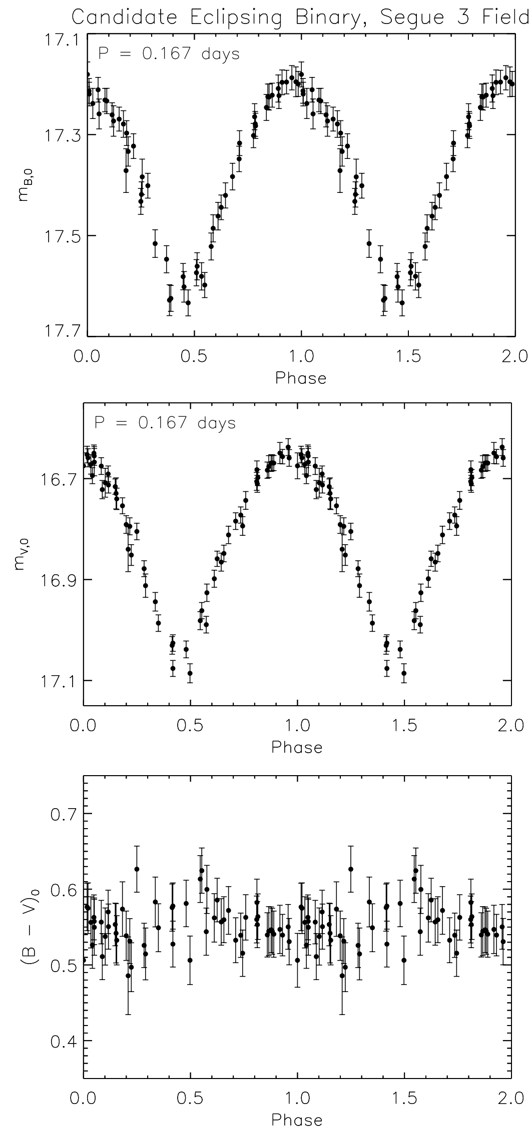

Figure 5. B_0 and V_0 light curves of a periodic variable star in the Segue 3 field are shown in the top and middle panels. These light curves are not well fit by the RRc light curve templates of Sesar et al. (2010), suggesting that this star is not an RRL candidate. The $(B - V)_0$ light curve shown in the bottom panel does not show clear variation as a function of phase and supports the hypothesis that this star is an eclipsing binary. The error bars include both random and systematic components.

Chaboyer (1999) gives the following relationship between absolute V band magnitude and metallicity for RRL stars:

$$M_{V,\mathrm{RR}} = (0.23 \pm 0.04)([\mathrm{Fe/H}] + 1.6) + (0.56 \pm 0.12). \quad (8)$$

Thus, we derive absolute magnitudes for the RRab star of $M_V = 0.43 \pm 0.14$ and $M_V = 0.37 \pm 0.15$ for metallicities of [Fe/H] = −2.16 and [Fe/H] = −2.44, respectively. Therefore, we find a distance to the RRab star of $d = 36.6^{+2.5}_{-2.4}$ kpc and $d = 37.7^{+2.7}_{-2.7}$ kpc. All of our distance measurements individually have ∼8% uncertainty and are consistent with literature values (see Belokurov et al. 2009 and Ripepi et al. 2012).

The distances to Segue 2 determined using both the RRL and BHB stars are consistent between the two techniques within one standard deviation. Note that this error budget does not include uncertainty in the metallicity of the RRL and BHB stars, nor the uncertainty in the absolute value of $E(B - V)$ at the location of the RRL star. If the reddening uncertainty is similar to the variation in SFD98 reddening across the face of Segue 2, this uncertainty may affect the inferred distance modulus by a couple hundredths of a magnitude (and thus the distance by ∼1%).

4. A CANDIDATE ECLIPSING BINARY IN THE SEGUE 3 FIELD

In the Segue 3 field, one periodic variable star was discovered at (RA, decl.) = ($21^{\mathrm{h}}21^{\mathrm{m}}41\overset{\mathrm{s}}{.}21$, $19°00'5\overset{''}{.}51$) at a distance of 17 half-light radii from the center of the object. The variable has a mean B band magnitude of $\langle m_B \rangle_0 = 17.407 \pm 0.018$ mag, a mean V band magnitude of $\langle m_V \rangle_0 = 16.862 \pm 0.013$ mag, and a mean color of $\langle B - V \rangle_0 = 0.550 \pm 0.004$. The star has a likely period of $P \sim 0.167$ days determined from a Lomb-Scargle periodogram. As shown in Figure 4, although the variable's apparent brightness is consistent with the horizontal branch of Segue 3, the star's color is more than 0.1 mag redder in $(B - V)_0$ than expected for an RRL star. Additionally, its light curves are not well fit by the RRc templates provided by Sesar et al. (2010). The variable's $m_{B,0}$, $m_{V,0}$, and $(B - V)_0$ light curves are shown in Figure 5.

The light curves of RRc stars and eclipsing binary star systems may appear deceptively similar in period, amplitude, and shape (Kinman & Brown 2010). However, while RRL stars vary in $B - V$ over the course of a pulsational period due to changes in effective temperature, an eclipsing binary system does not show significant variation in $B - V$ (see, e.g., Figures 4–6 of Kinman & Brown 2010). As shown in Figure 5, the variable star does not show clear variation in $(B - V)_0$ as a function of phase, suggesting that this variable may be an eclipsing binary.

5. CONCLUSIONS

We have used multi-band time-series photometry obtained at the WIYN 0.9 m telescope at KPNO to conduct a complete search for RRL stars in Segue 2 and Segue 3. We have discovered an RRL star with properties consistent with a fundamental mode RRL (RRab) star in Segue 2, and a candidate eclipsing binary in the Segue 3 field. We derive the first robust distance to Segue 2 using both its RRL star and spectroscopically confirmed BHB stars. The latter method yields a distance of $d = 34.4 \pm 2.6$ kpc (for [Fe/H] = −2.257), while the former method gives distances of $d = 36.6^{+2.5}_{-2.4}$ kpc and $d = 37.7^{+2.7}_{-2.7}$ kpc for [Fe/H] = −2.16 and −2.44, respectively. These distances are consistent with one another to within one standard deviation. Future spectroscopic measurements of the RRab and the BHB stars' [Fe/H] will facilitate an even more robust measurement of the distance to Segue 2.

We revisit the known anti-correlation between $\langle P_{\mathrm{ab}} \rangle$ and $\langle$[Fe/H]$\rangle$ for RRL in Milky Way dwarf galaxies, using a uniformly calculated set of $\langle$[Fe/H]$\rangle$ and $\langle P_{\mathrm{ab}} \rangle$. Placing the 0.748 day period of the Segue 2 RRab star in this context, we find that the RRab period and mean metallicity of Segue 2 are consistent with the established trend given the significant spread in metallicity in Segue 2 demonstrated by Kirby et al. (2013). The tightness of the observed inverse correlation between $\langle P_{\mathrm{ab}} \rangle$ and $\langle$[Fe/H]$\rangle$ in dwarf galaxies is worthy of careful, continued study as more RRL are found in these objects. This relation may ultimately yield an interesting avenue for inference of the chemical properties of diffuse streams and distant ultra-faint dwarfs in the era of time domain surveys such as LSST.

E.B., B.W., R.F., M.B., and E.H. acknowledge support from NSF AST-0908193 and NSF AST-1151462. E.B., T.T.A., E.C.C., T.D., J.G., A.P., and A.P.S. acknowledge observatory travel support from Haverford College's Green Fund. We thank Branimir Sesar, Gisella Clementini, Dustin Lang, and Marla Geha for helpful comments and conversations, and Scott Engle for his help with data collection. We thank Joshua Haislip for providing a Python script for interfacing with Astrometry.net. We acknowledge Haverford's Koshland Integrated Natural Sciences Center for supporting WIYN 0.9 m membership dues. We thank Joe Cammisa for his computing support and Hillary Mathis for training us to use the WIYN 0.9 m telescope and S2KB camera. We also thank the anonymous referee for very helpful comments. This work has made use of NASA's Astrophysics Data System.

REFERENCES

Abazajian, K. N., Adelman-McCarthy, J. K., Agüeros, M. A., et al. 2009, ApJS, 182, 543
Alcock, C., Allsman, R. A., Alves, D. R., et al. 2000, AJ, 119, 2194
Belokurov, V., Walker, M. G., Evans, N. W., et al. 2008, ApJL, 686, L83
Belokurov, V., Walker, M. G., Evans, N. W., et al. 2009, MNRAS, 397, 1748
Belokurov, V., Walker, M. G., Evans, N. W., et al. 2010, ApJL, 712, L103
Belokurov, V., Zucker, D. B., Evans, N. W., et al. 2006, ApJL, 647, L111
Belokurov, V., Zucker, D. B., Evans, N. W., et al. 2007, ApJ, 654, 897
Bersier, D., & Wood, P. R. 2002, AJ, 123, 840
Bonanos, A. Z., Stanek, K. Z., Szentgyorgyi, A. H., Sasselov, D. D., & Bakos, G. Á. 2004, AJ, 127, 861
Cacciari, C., & Clementini, G. 2003, in Stellar Candles for the Extragalactic Distance Scale, ed. D. Alloin & W. Gieren (Lecture Notes in Physics, Vol. 635; Berlin: Springer), 105
Catelan, M. 2009, Ap&SS, 320, 261
Chaboyer, B. 1999, Post-Hipparcos Cosmic Candles, Vol. 237 (Dordrecht: Kluwer), 111
Clement, C. M., Muzzin, A., Dufton, Q., et al. 2001, AJ, 122, 2587
Clementini, G. 2010, in Variable Stars, the Galactic Halo and Galaxy Formation, ed. C. Sterken, N. Samus, & L. Szabados (Moscow: Sternberg Astronomical Institute of Moscow University), 107
Dall'Ora, M., Clementini, G., Kinemuchi, K., et al. 2006, ApJL, 653, L109
Dall'Ora, M., Kinemuchi, K., Ripepi, V., et al. 2012, ApJ, 752, 42
Fadely, R., Willman, B., Geha, M., et al. 2011, AJ, 142, 88
Foreman-Mackey, D., Hogg, D. W., Lang, D., & Goodman, J. 2013, PASP, 125, 306
Garofalo, A., Cusano, F., Clementini, G., et al. 2013, ApJ, 767, 62
Greco, C., Dall'Ora, M., Clementini, G., et al. 2008, ApJL, 675, L73
Held, E. V., Clementini, G., Rizzi, L., et al. 2001, ApJL, 562, L39
Jordi, K., Grebel, E. K., & Ammon, K. 2006, A&A, 460, 339
Kaluzny, J., Kubiak, M., Szymanski, M., et al. 1995, A&AS, 112, 407
Kinman, T. D., & Brown, W. R. 2010, AJ, 139, 2014
Kirby, E. N., Boylan-Kolchin, M., Cohen, J. G., et al. 2013, ApJ, 770, 16
Kirby, E. N., Guhathakurta, P., Simon, J. D., et al. 2010, ApJS, 191, 352
Kirby, E. N., Simon, J. D., Geha, M., Guhathakurta, P., & Frebel, A. 2008, ApJL, 685, L43
Koposov, S., de Jong, J. T. A., Belokurov, V., et al. 2007, ApJ, 669, 337
Koposov, S. E., Gilmore, G., Walker, M. G., et al. 2011, ApJ, 736, 146
Kuehn, C., Kinemuchi, K., Ripepi, V., et al. 2008, ApJL, 674, L81
Kunder, A., Walker, A., Stetson, P. B., et al. 2011, AJ, 141, 15
Mateo, M., Fischer, P., & Krzeminski, W. 1995, AJ, 110, 2166
Miceli, A., Rest, A., Stubbs, C. W., et al. 2008, ApJ, 678, 865
Moretti, M. I., Dall'Ora, M., Ripepi, V., et al. 2009, ApJL, 699, L125
Muñoz, R. R., Geha, M., Côté, P., et al. 2012, ApJL, 753, L15
Musella, I., Ripepi, V., Clementini, G., et al. 2009, ApJL, 695, L83
Musella, I., Ripepi, V., Marconi, M., et al. 2012, ApJ, 756, 121
Nemec, J. M., Wehlau, A., & Mendes de Oliveira, C. 1988, AJ, 96, 528
Norris, J. E., Wyse, R. F. G., Gilmore, G., et al. 2010, ApJ, 723, 1632
Oosterhoff, P. T. 1939, Obs, 62, 104
Ripepi, V., Mancini, D., Cortecchia, F., et al. 2012, MSAIS, 19, 152
Sand, D. J., Strader, J., Willman, B., et al. 2012, ApJ, 756, 79
Sarajedini, A., Barker, M. K., Geisler, D., Harding, P., & Schommer, R. 2006, AJ, 132, 1361
Schlafly, E. F., & Finkbeiner, D. P. 2011, ApJ, 737, 103
Schlegel, D. J., Finkbeiner, D. P., & Davis, M. 1998, ApJ, 500, 525
Sesar, B., Ivezić, Ž., Grammer, S. H., et al. 2010, ApJ, 708, 717
Sesar, B., Ivezić, Ž., Lupton, R. H., et al. 2007, AJ, 134, 2236
Siegel, M. H. 2006, ApJL, 649, L83

Siegel, M. H., & Majewski, S. R. 2000, AJ, 120, 284
Simon, J. D., Geha, M., Minor, Q. E., et al. 2011, ApJ, 733, 46
Smith, H. A. 1995, RR Lyrae Stars (Cambridge: Cambridge Univ. Press)
Smith, H. A., Catelan, M., & Clementini, G. 2009, in AIP Conf. Proc. 1170, Stellar Pulsation: Challenges for Theory and Observation, ed. J. A. Guzik & P. A. Bradley (Melville, NY: AIP), 179
Stetson, P. B. 1987, PASP, 99, 191
Stetson, P. B. 1994, PASP, 106, 250
Vivas, A. K., Zinn, R., Abad, C., et al. 2004, AJ, 127, 1158
Walsh, S. M., Jerjen, H., & Willman, B. 2007, ApJL, 662, L83
Willman, B., Blanton, M. R., West, A. A., et al. 2005a, AJ, 129, 2692
Willman, B., Dalcanton, J. J., Martinez-Delgado, D., et al. 2005b, ApJL, 626, L85
Willman, B., Geha, M., Strader, J., et al. 2011, AJ, 142, 128
Willman, B., & Strader, J. 2012, AJ, 144, 76
Wolf, J., Martinez, G. D., Bullock, J. S., et al. 2010, MNRAS, 406, 1220
Zucker, D. B., Belokurov, V., Evans, N. W., et al. 2006a, ApJL, 650, L41
Zucker, D. B., Belokurov, V., Evans, N. W., et al. 2006b, ApJL, 643, L103